Journal of Applied Polymer Science

# A methodology for fabrication of thermomechanically activated switchable surface wettability

**Christopher M. Laursen,[1] Jonathan A. Brant,[2] Carl P. Frick[1]**
[1]Department of Mechanical Engineering, University of Wyoming, 1000 E. University Avenue, Laramie, Wyoming 82071
[2]Department of Civil and Architectural Engineering, University of Wyoming, 1000 E. University Avenue, Laramie, Wyoming 82071
Correspondence to: C. M. Laursen (E-mail: claursen@uwyo.edu)

**ABSTRACT:** In this study a platform is laid out for the creation of a multitiered surface exhibiting switchable wettability. This is done through a combination of both an acrylate-based polymer understructure photopolymerized into a pillared array, and selectively placed surface treatments on these pillars. The acrylate-based polymer is created through a systematic study and is shown to exhibit drastic alterations in material stiffness over a 19 °C temperature transition under aqueous conditions, allowing for stiff, erect pillars in the low temperature state, and pliable pillars that can easily be bent in the high temperature state. The glass transition temperature and onset temperature for the polymer system is found to be 49 and 30 °C, respectively. Three different surface treatments, including trichloro(1H,1H,2H,2H-perfluorooctyl)silane, polydimethylsiloxane, and polydopamine, are investigated using static contact angle studies, and are selectively deposited onto the pillared surface such that a hydrophobic surface is exposed with the pillars erect, and a hydrophilic surface is exposed with the pillars in the bent state. The surface is shown to transition between first a hydrophobic, then hydrophilic state and return to a hydrophobic state when the investigations are coupled together forming a hierarchical surface structure. © 2016 Wiley Periodicals, Inc. J. Appl. Polym. Sci. **2016**, *133*, 44122.

**KEYWORDS:** biomimetic; copolymers; glass transition; properties and characterization; surface and interfaces

Received 21 March 2016; accepted 21 June 2016
**DOI: 10.1002/app.44122**

## INTRODUCTION

Research interest in altering of surface properties, especially the wettability characteristics, has surged in recent years because of demand for various applications. Applications requiring alterations in wettability characteristics from the materials substrate can include self-cleaning, antifouling, or low friction surfaces, microfluidics, waterproof textiles, and a range of other fields.[1–6] Generally, modifications have been made to alter the surface's hydrophobic/hydrophilic character of a material using two techniques; by morphological, chemical, or a combination thereof. Although using these listed techniques has the benefit of being able to change characteristics from the bulk material, without an additional component these materials are locked into their set wettability.

Common chemical modifications of interest for example may include the use of poly(ethylene glycol) grafted chains,[2] plasma treatment methods,[7–10] or the use of self-assembled monolayers.[11,12] Some modifications, such and pol(ethylene glycol) grafting and self-assembled monolayers coat the surface via chemical reactions, while plasma treatment chemically alters the already present surface. However, all of these methods have the overarching goal of altering the surface energy to influence chemical interactions. For example, poly(ethylene glycol) chains have been shown to be an effective surface coating by resisting proteins through steric repulsions, van der Waals forces, and hydrophobic interactions.[13]

An additional approach to altering surface characteristics is through a morphological method, that is, creating structured surfaces. This idea originated from observations of debris deposition on "super-hydrophobic" surfaces in nature, which include lotus leaves and shark skin.[1,14–20] From these observations a variety of synthetic, "super-hydrophobic" surfaces have evolved. Original developments explaining this phenomenological effect were based off the development of a Cassie–Baxter state and Wenzel states, that is, solid–liquid–gas interface.[21–24] Work by Nosonovsky and Bhushan attempted to optimize the best morphological structure, finding cylindrical structures in hexagonal arrays are an appropriate choice.[16]

More recently, switchable wettability surfaces have been realized and have been the focus of increased interest due to their ability to add additional functionality to surfaces such as applications in self-cleaning surfaces, reversible adhesion, and microfluidics.[25–28] These materials have characteristics leaving them now

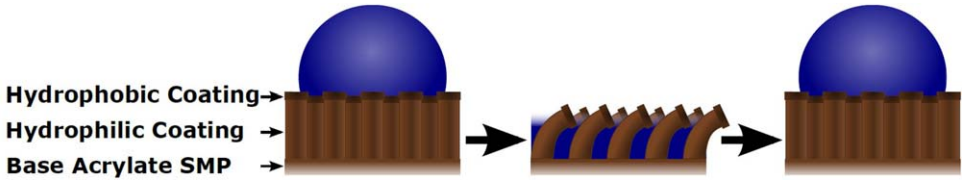


**Figure 1.** Schematic of proposed structure starting in its hydrophobic state followed by heating coupled with a small load, becoming hydrophilic, and then returning to its hydrophobic state upon removal of the load and cooling. [Color figure can be viewed in the online issue, which is available at wileyonlinelibrary.com.]

not locked into one state but instead allow for switchable "smart" surfaces that, under the alteration of a stimulus (e.g., chemical reaction, light, temperature), alter the parameters of wettability. Most research examples using stimuli to affect the hydrophobicity/hydrophobicity of surfaces a centered around modification of the chemical structure, either by light,[25,29] counter ion exchange,[30] electrical potential alterations,[31] and through thermal effects.[12,32–35] However, very few investigators have also considered using a morphological approach to switch surface wettability.[36–38] One example is through a liquid crystal elastomer that transitions from a nematic to isotropic state as a function of temperature.[36] Others have used mechanical excitation to transition from a 'rippled state' to a flat state using surface treated polydimethylsiloxane (PDMS).[37] In addition, similar to the study here, Chen and Yang have created a switchable pillared surface in which they deform to change the surface wettability, but instead out of an epoxy resin.[38] Currently, the biggest drawback to the use of these techniques is the inherent difficulty in altering the transition behavior to fit the needs of the environment the material is to operate in, that is, tailor the transition temperature to fit the needs of the application.

In this article, we demonstrate a methodology for fabrication of a unique, multitiered platform displaying a switchable hydrophilic and hydrophobic property through a *combination* of preferentially altered surface chemistry, surface morphology, and through the use of a thermally activated smart-polymer substructure. Figure 1 demonstrates the premise of the multitiered system, showing the proof-of-concept design. Labeled on the figure is smart-polymer acrylate structure, which has been cast into a pillared array. A hydrophilic coating has been selectively deposited on the smart-polymer's surface everywhere except on the tops, which instead has been treated with a hydrophobic coating. In the surface's unaltered state, the material exhibits a hydrophobic nature. Through sufficiently heating the acrylate-based polymer, the system becomes pliable, and under a small load the pillars bend, exposing the hydrophilic nature. Subsequently the surface can be returned to its unaltered, hydrophobic state, by removing the force and retuning to lower temperature operating conditions.

The path used in this research was a ground-up approach, first customizing a photopolymerizable shape memory polymer system. It was advantageous in this case to create a custom designed smart-polymer system via a systematic study in which the thermo-mechanical properties can easily be altered because it allowed for a more robust system that can be custom tailored to fit the needs of future applications. For example, the smart-polymer system chemistry can be altered to systematically control the glass transition temperature, thereby causing a shift in thermomechanical behavior, and the surface geometry can easily be modified to different patterning and size scales from the μm to mm range.

For this study, the acrylate-based polymer system was chosen from a large family of commercially available macromolecules. The inherent benefit in the choice of these materials includes their proven shape memory characteristics when tailored correctly. However, they also have the advantages of being biocompatible, having a diverse variety of functional groups allowing for a range of wetting characteristics and glass transitions, and they have the ability to be photopolyermized through the free-radical chain-polymerization process, allowing for a large range of shapes and size scales.[39–42]

Similarly, a modifiable approach was also considered when choosing various surface treatments and application methods so that treatments could also be spatially varied on the pillared structure. The research performed here considers two main chemical surface modifications, polydopamine (PDOPA) and trichloro(1H,1H,2H,2H-perfluorooctyl)silane (PFOS) to alter the surfaces hydrophilicity and hydrophobicity of the smart-polymer surface, respectively.

Polydopamine (PDOPA) is a biologically inspired surface coating found, among other uses, to enhance surface hydrophilicity. Early investigations into dopamine were based off observations of adhesive proteins secreted by *Mytilus edulis*, a marine mussel.[43] Through the complex and various chemical combinations created during of polymerization of dopamine, the coating has been found to readily adhere when polymerized on a variety of substrates from metals, to ceramics, to polymers and was initially shown as a possible hydrophilic coating amongst other uses by Lee *et al.*[44] Further work by Liao and company sought to quantify the effects of deposition time, dopamine concentration in solution, and solution alkalinity to maximize the hydrophilicity on polyimide films. Ultimately these researchers achieved static contact angles as low as 46°.[45] The hydrophilic character and robustness of the coating can be attributed to both its catechol and amine functional groups within the polymer precursor. The polymerization of the substance can go through many different chemical processes to bind to a surface as seen in a review by Liu, Ai, and Lu, but what remains after polymerization typically are two polarized hydroxyl groups per repeat unit.[5] These hydroxyl groups can subsequently be used as binding sites for other chemical processes or used to increase hydrophilicity.

| | Material | Structure | Molecular Weight (g/mol) |
|---|---|---|---|
| (a) | tert-Butyl acrylate (tBA) | 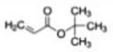 | 128.17 |
| (b) | 2-Ethoxyethyl methacrylate (2EEM) | 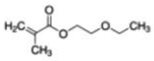 | 158.19 |
| (c) | Poly(propylene glycol) acrylate (PPGA) | 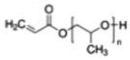 | ~475 |
| (d) | 2-Carboxyethyl acrylate (2CEA) | 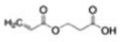 | 144.13 |
| (e) | 2-Hydroxyethyl methacrylate (2HEMA) | 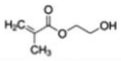 | 130.14 |
| (f) | Di(ethylene glycol) dimethacrylate (DEGDMA) | 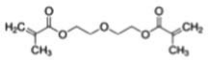 | 242.27 |
| (g) | Poly(ethylene glycol) dimethacrylate $M_n$ 550 (PEGDMA550) | 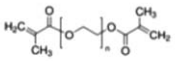 | ~550 |
| (h) | Poly(ethylene glycol) dimethacrylate $M_n$ 750 (PEGDMA750) | 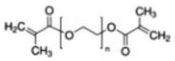 | ~750 |
| (i) | Dipentaerythritol penta-/hexa-acrylate (DPPHA) | 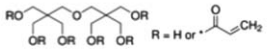 | 524.51 |
| (j) | 2,2-Dimethoxy-2-phenyl -acetophenone (DMPA) | 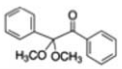 | 256.3 |

**Figure 2.** Name, structure, and molecular weight of (a–e) monofunctional acrylates, (f-i) multifunctional acrylates, and (j) photoinitiator.

On the opposite spectrum, trichloro(1H,1H,2H,2H-perfluorooctyl)silane (PFOS) is a self-assembled layer having a hydrophobic surface chemistry after polymerization. Through deposition of this self-assembled layer, the precursor chemically binds via hydration of the chlorosilane groups followed by polymerization leaving an exposed fluoroalkyl functional group on the surface and bound together siloxane groups.[46,47] The Chen group, initially proposing the method for molding techniques, also found that the system can further be enhanced through an annealing process, lowering the surface energy from approximately 26 mJ/m$^2$ to around 7 mJ/m$^2$ when treated at 150 °C for 1 hr.[47] Note also that the PFOS surface treatment has not only been found to be effective for use in molding processes,[47,48] but also for making surfaces more hydrophobic.[31,49] Though various mechanisms for self-assembly of the PFOS have been proposed, a modified method based off Rajkumar and Rajendrakumar's work was proved most successful in this research.[31]

## EXPERIMENTAL

### Materials

The following materials for the polymer network were procured from Sigma-Aldrich Corporation, St. Louis, MO. Macromolecules tert-Butyl acrylate (tBA), 2-ethoxyethyl methacrylate (2EEM), poly(propylene glycol) acrylate (PPGA), 2-carboxyethyl acrylate (2CEA), di(ethylene glycol) dimethacrylate (DEGDMA), poly(ethylene glycol) dimethacrylate $M_n$ 550 (PEGDMA550), poly(ethylene glycol) dimethacrylate $M_n$ 750 (PEGDMA750), and photo-initiator 2,2-dimethoxy-2-phenyl-acetophenone (DMPA). Additional macromolecules, 2-hydroxyethyl methacrylate (2HEMA) and dipentaerythritol penta-/hexa-acrylate (DPPHA) were obtained through Alpha Aesar, Ward Hill, MA, and Santa Cruz Biotechnology Incorporated, Santa Cruz, CA, respectively. The chemical structure, molecular weight, and acronym used for each macromolecule investigated can be found in Figure 2.

In order to apply the various surface treatments to the tailored polymer system, the following items were required. The two-part system for Sylgard 184 silicone elastomer (PDMS) from Dow Corning Corporation, Midland, MI was used alone to create a hydrophobic surface. An additional hydrophobic surface treatment could be produced using trichloro(1H,1H,2H,2H-perfluorooctyl)silane (PFOS) and hexane procured from Sigma-Aldrich Corporation. In addition, Trizma® hydrochloride (pH buffer), and dopamine hydrochloride, also procured from Sigma-Aldrich Corporation, could be used to create a hydrophilic surface.

### Polymer Synthesis

**Individual Acrylate Systems.** Fundamental studies of the basic macromolecules were prepared for photo-initiated chain polymerization through the addition of 0.5 wt % DMPA photo-initiator in all cases. Additionally, the five monofunctional acrylates seen in Figure 2 were crosslinked for mechanical testing through the addition of 1 wt % DEGDMA such that the final linear-builder based systems consisted of 98.5 wt % respective monofunctional macromolecule, 1 wt % DEGDMA, and 0.5 wt % DMPA. These samples were prepared in 5 g batches. After mixing the proper ratios, samples were subsequently shaken by hand for 2 min and ultrasonically shaken in a Branson

1510 Ultrasonic Cleaner for 5 min to ensure complete dispersion of constituents. Samples were stored at 5 °C away from light until cast.

**Final Ternary Acrylate System.** Initial investigations of the individual polymer constituents resulted in a final ternary network consisting of a linear building mixture of 9:1 by weight tert-Butyl acrylate to 2-hydroxyethyl methacrylate (tBA and 2HEMA respectively), which was subsequently mixed with a multifunctional (crosslinking) system, poly(ethylene glycol) dimethacrylate $M_n$ 550 (PEGDMA550), and a photo-initiator, 2,2-dimethoxy-2-phenyl-acetophenone (DMPA) such that final composition consisted of 94.5/5.0/0.5 wt % linear building mixture, PEGDMA550, and DMPA. The final relative weight percentage of each constituent overall was 85.05/9.45/5.00/0.50 wt % tBA, 2HEMA, DEGDMA, and DMPA. Materials were mixed together in approximately 100 g batches as needed and mixed using the method described in the previous section. The mixture was once again stored in a UV-resistant vial and placed in a refrigerator at 5 °C out of the light.

**Thermo-Mechanical Sample Casting.** Both Dynamic Mechanical Analysis (DMA) and tensile samples were cast in a similar method using the mixture of interest prepared above, just with different polytetrafluoroethylene (PTFE) spacer molds. To prepare the molds, first Rain-X® release agent was applied to two pre-cleaned plain glass microscope slides. A thin layer of vacuum grease was applied to the contact regions between the PTFE spacer and the glass, and the pieces were sandwiched and clamped together. The uncured mixture of interest was then injected in between the slides. Photopolymerization was induced using a 365 nm wavelength UV lamp (UVP Blak-Ray B-100A/R lamp, intensity ~8 mW/cm$^2$) for approximately 30 min. Subsequently the samples were placed into a furnace (Fisher Scientific Isotemp) at 90 °C for 60 min to ensure complete polymerization. Samples were finalized for DMA or tensile testing by trimming and sanding samples edges.

### Thermo-Mechanical Testing

**Water Absorption Studies.** Water absorption studies were performed on polymerized samples cut into approximately 10 × 10 mm$^2$ squares after casting approximately 1 mm thick. Tests were run using water obtained from a Millipore Direct-Q system over duration of 10 days at room temperature, with observations being taken on periodical intervals, lengthening as time increased. Before submersion all sample's dry masses were taken. At the time interval of interest, samples were removed from the water, dabbed with a wipe so there was no standing water on the surface, and the samples were massed. Knowing these two masses, the percentage of absorbed water could be observed.

**Dynamic Mechanical Analysis.** DMA was performed on a TA Instruments Q800 DMA affixed with film tensile grips. PTFE molds were approximately 1 mm thick, and had cutouts for 15 × 6 mm$^2$ samples. The sample's final dimensions were measured immediately before placing into the DMA. Samples created from the ternary networks were investigated in both dry and soaked conditions. To model the polymer's behavior under submerged conditions, samples were first soaked for 24 hr before testing. In addition, to minimize water loss during testing at high temperatures, samples were coated in a layer of vacuum grease.

Tests was performed under a strain controlled temperature sweep between the temperatures of interest ramped at 1 °C/min and a frequency of 1 Hz. Observed temperature ranges depended on the sample of interest, and were started as low as −50 °C and ended as high as 200 °C. Temperature testing ranges for the final ternary polymer system when soaked were between 0 and 100 °C. Preload force, target strain, and force track were held constant at 0.1 *N*, 0.1, and 150%, respectively. In order to assure equilibrium between the sample and thermal chamber, the test sequence also included initially flooding the system with liquid nitrogen until 20 °C below the initial data acquisition temperature was reached. At that point, the sequence was held isothermally for 5 min, and then begun ramping at 1 °C/min until the data acquisition starting temperature was met, where normal operation commenced. Measured properties included temperature, cyclic input force, and resultant displacement, along with phase lag between these two. The latter three measurements were used to calculate the storage and loss moduli along with tan delta.

**Tensile Testing.** Tensile testing was performed on the final ternary polymer network consisting of 94.5 wt % 9:1 tBA-co-2HEMA, 5 wt % PEGDMA550, and 0.5 wt % DMPA. Samples were cast using the method described in the section, *Thermo-Mechanical Sample Casting*, such that the PTFE dog-bone mold had an overall length of 63.5 mm (2.50 in.), width of 9.53 mm (0.375 in.), gage width of 3.18 mm (0.125 in.), and a gage length of 12.7 mm (0.50 in.). Samples were approximately 3.2 mm thick before final preparatory work. Final measurements were taken immediately before testing.

Testing was performed on a MTS 858 Mini Bionix II servo-hydraulic load frame affixed with a MTS 407 Controller; though data acquisition and control was applied through an in-house LabView program. Force was typically measured with a MTS 661.09B-21 100 *N* force transducer and routed through the 407 Controller while displacement was measured via an MTS LX 500 Laser Extensometer using retro-reflective tape placed on the gage length of the sample. To control signal to noise ratio with a decrease in overall mechanical properties at higher temperatures, samples tested at 90 °C used a Transducer Techniques MLP-10 10lb$_f$ force transducer. The load frame was enclosed in a MTS 651 Environmental Chamber with both liquid nitrogen cooling and two electric heating elements coupled with a fan for diffused convective heating. Temperatures for testing ranged from 10 to 90 °C. As with DMA testing, all samples were massed and measured immediately before testing if soaked. Testing was completed at a strain rate of 0.1% sec$^{-1}$ and data acquisition of 2 Hz.

### Surface Treatments

Multiple surface treatments were investigated to allow for a selection of hydrophobic and hydrophilic surface characteristics. Samples were investigated for wettability using a Krüss DSA25 goniometer to measure static contact angle with water (Millipore Direct-Q) as the media. All surface treatments were tested

on the final acrylate system, and were cast in a similar method to that described in the casting section, with release agent only being applied to one side. This produced a flat sheet of acrylate cast onto a glass backing. Samples were then scrubbed with soap and flushed with ultra-pure water followed by isopropyl alcohol. Samples were deposited with the surface treatments described below, and were soaked for 24 hr in water, representing conditions under submerged applications. Immediately before testing contact angle, sample surfaces were dabbed so no residual water was left on the surface. Five to seven measurements were taken on each sample with a 10 μL drop using the one-tangent method.

Previous studies of dopamine hydrochloride have been shown to self-polymerize into polydopamine (PDOPA) under slightly basic aqueous solutions. Previous groups have investigated deposition under two different solutions; with a pH of 8.5 used by Lee *et al.*,[44] and a pH of 8.8 used by McCloskey *et al.*[50,51] Effects of the deposition time when applied on our material were tested here with the samples being prepared with a pH between 8.5 and 8.8 as follows.

Water in 45 mL batches first had a solute of Trizma® hydrochloride added as a pH buffer in a 10–15 m*M* solution with the goal of adjusting the solution to a pH between 8.5 and 8.8. The pH of the solution was adjusted using drops of 1 *N* (Eq/L) and 0.1 *N* solution of sodium hydroxide. Once the pH solution was prepared accordingly, 2 mg/mL of dopamine hydrochloride were added to a 50 mL test beaker with samples attached vertically along the wall. Polymerization of the surface coating was conducted in an open-air environment and stirred continuously at 250 RPM at room temperature. Separate test samples were deposited for durations of 2, 4, 8, and 24 hr for contact angle observation. Once the surface deposition was completed at the correct time interval, the samples were rinsed heavily with water and placed in a desiccator to dry.

Trichloro(1H,1H,2H,2H-perfluorooctyl)silane (PFOS) is a fluorinated chlorosilane precursor that could be polymerized into a self-assembled monolayer and be used as a hydrophobic surface treatment, as well as a release agent in the molding process. Different molarities as well as annealing temperatures were tested in this investigation including 5, 10, 15, and 20 m*M* solutions, and at 90 and 150 °C post-deposition annealing temperatures. To begin treatment, a select molarity solution of PFOS in hexane was mixed and placed in the ultrasonic cleaner for 5 min. Samples were then submerged into the solution, and placed in the refrigerator to allow for self-assembly. After 20 min, samples were removed from the solution and rinsed heavily with hexane to remove any loosely bonded PFOS. Samples were finished curing in an open air furnace (Fisher Scientific Isotemp) at either 90 or 150 °C for 60 min, annealing the coating.

Polydimethylsiloxane (PDMS), has also been investigated heavily as a standalone hydrophobic surface, and can easily be extended for our research here for use as a coating on the acrylate based structure.[17,52–54] Flat sheet samples were hand mixed in a 10:1 weight ratio of base to curing agent and poured into simple weigh boats. The mixture was then degassed and placed in an oven at 90 °C to cure for 1 hr. Contact angle studies were performed on the top surface after being cleaned with water.

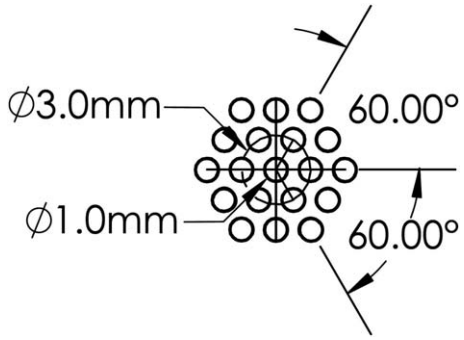


**Figure 3.** Schematic of the hexagonal pillar-patterning. In addition, pillars were 3 mm tall, not reflected in the figure.

**Patterned Surface Molding**

Molds were machined from blocks of polyoxymethylene polymer in-house. Well dimensions for pillar backing were 1 cm by 4 cm. The mold also contained a 3:1 hexagonal packing factor between centers based off of the hole diameter. Holes were 1 mm in diameter and 3 mm deep. This pattern is reflected in Figure 3.

To ensure the acrylate network would not adhere to the surface, molds first needed to be coated with a self-assembled film of trichloro(1H,1H,2H,2H-perfluorooctyl)silane to act as a release agent. Treatment for self-assembling the layer was similar to that described in the section, *Structured Surface Treatments*. A 10 m*M* solution of PFOS in hexane was mixed in a 5 mL batch and placed in the ultrasonic cleaner for 5 min immediately before placing into the mold. The molds were next degassed to remove entrapped air in the pillar holes and placed the refrigerator. After 20 min, samples were removed from the solution and rinsed heavily with hexane and cured at 90 °C to anneal the layer.

With the self-assembled coating polymerized on the mold surface the final ternary polymer structure could be cast in the mold. The acrylate was first precured in a 254 nm wavelength crosslinking oven (Spectrolinker XL-1500 intensity ~1.5 mW/cm$^2$, Spectronics Corporation) for 20 min. A glass slide was placed over the mold top with a vacuum grease seal, and the partially cured polymer was injected. Following this the system was placed in at a slight incline, and vacuum desiccated at 300 Torr for 45 min, or until no bubbles were seen to escape. Polymerization was finished under a 365 nm wavelength UV lamp for and additional 10 min and subsequently placed in an oven at 90 °C for 60 min. The method allowed for simple delamination from the mold at elevated temperatures.

**Multitier Structure Surface**

After the final acrylate structure was cast, selectively placed surface treatments were added to the structure. First, the entire surface was subjected to PDOPA treatment, polymerized in a pH solution of 8.5 for 24 hr, subsequently being rinsed in water and dried, as discussed previously. This created a hydrophilic surface over the entire acrylate structure. To create the

**Table I.** Water Absorption and Thermo-Mechanical Properties of Base Acrylate Systems

| | Acrylate | Water absorption (wt %) | Onset temperature (°C) | Glass transition temperature (°C) | Glassy modulus (MPa) | Rubbery modulus (MPa) |
|---|---|---|---|---|---|---|
| (a) | tBA | 0.9 ± 0.5 | 38 ± 1.4 | 46.5 ± 1.8 | 1700 ± 100 | 2.3 ± 0.6 |
| (b) | 2EEM | 1.7 ± 0.7 | — | 30.9 | 1400 | 1.9 |
| (c) | PPGA | −6.0 ± 2.7 | — | −48.5 | — | — |
| (d) | 2CEA | — | 26 | 42.3 ± 0.3 | 3400 ± 2000 | 1.2 ± 0.4 |
| (e) | 2HEMA | 54 ± 1 | 83.0 ± 4.0 | 120.5 ± 0.1 | 4100 ± 1600 | 6 ± 5 |
| (f) | DEGDMA | 3.5 ± 1.2 | — | — | — | — |
| (g) | PEGDMA550 | 21 ± 2 | — | 4.1 ± 0.5 | — | 64 ± 3 |
| (h) | PEGDMA750 | 44 ± 3 | — | −31.5 ± 0.3 | — | 29 ± 1 |
| (i) | DPPHA | 3.4 ± 0.4 | — | — | — | — |

hydrophobic pillar tops, samples were either dip coated in PDMS, producing a flanged top, or deposited with PFOS.

The process for pillars cast with PDMS flanged tops used the following procedure. First, the pillar surfaces were sanded ensuring pillar tops would be completely uniform along their top plane and were cleaned using water and dried. This was followed by preparing the PDMS through mixing the two base constituents in a 10:1 weight ratio as per manufacturer recommendation, and spin casting 1.5 g in a petri dish at 200 RPM for 10 min. The structured surfaces could then be dipped into the thin PDMS coating, carefully placed on to a Rain-X® coated aluminum sheet, and cured at 90 °C for 60 min. Samples were cooled, removed, and the process was repeated three more times, producing uniformly distributed flanges that were not touching each other. This method is similar to that used by Hossfeld *et al.*[55]

Alternatively, to deposit a self-assembled PFOS hydrophobic layer, pillar tops were submerged between 0.5 and 1 mm deep in a 10 m*M* PFOS solution with hexane for 20 min at 5 °C. The samples were subsequently rinsed heavily with hexane, and placed in the oven to anneal at 150 °C for 1 hr. Further detail on the deposition process can be found in the section, *Structured Surface Treatments.*

## RESULTS

### Base Polymer Systems

Initially, the nine acryl-based macromolecules were investigated both for their thermo-mechanical behavior as well as water absorption. This information would later be used to isolate an optimal combination of macromolecules that, when polymerized, exhibit the desired aqueous glass transition behavior, water absorption, and mechanical properties. A final polymer system was required to first exhibit good shape-memory properties in aqueous media, targeted for a glass onset temperature ($T_{on}$) of approximately 30–45 °C under submerged conditions. It also needed appropriate high and low temperature mechanical properties including strain-to-failure and mechanical toughness. Finally, it required the ability to be photopolymerized into a structured surface. With this future in mind, it was imperative to first understand the characteristics of the initial systems individually. Of the nine initial systems, five of them were monofunctional (linear-builders), while the remaining four were multifunctional (crosslinking) molecules as shown in Figure 2.

The water absorption of each individual polymer system was observed through the use of eq. (1), where $M_d$ and $M_w$ represent the dry and wet masses respectively taken before soaking and immediately after removal at the selected interval. Water absorption should be affected by the amount of free volume in the polymer as well as the chemical composition of the acryl side groups. As the final product is targeted for aqueous environment, it was important to fundamentally understand the individual water absorption rates and saturation points of each polymer group being considered.

$$\%_{abs} = \left(\frac{M_w - M_d}{M_d}\right) * 100 \quad (1)$$

In addition, initial dynamic thermo-mechanical testing of dry samples was performed using DMA to observe each constituent's glass transition temperature, onset transition temperatures, and storage moduli in the rubbery and glassy regimes. For the purposes of this study, the glass transition temperature ($T_g$) is defined as the peak of the tan delta curve, while the onset temperature ($T_{on}$) is defined as the intersection of two lines laid tangent to the glassy region and the transition regions when observing the storage moduli curve.

Highlights of these results can be seen in Table I, displaying the glass and rubbery transition temperatures, storage moduli in both the glassy and rubbery regimes, and the weight percent water absorption at 10 days for the initial systems. Voids in the table represent unobtainable data; missing onset temperatures, glass transition temperatures, and moduli were a result of an ill-defined glassy regime and/or transition regions in the tested system, while materials that lack water absorption data dissolved into solution within the observation period.

For the linear builders, water absorption ranged from 53.8 ± 1.2 wt % to 0.94 ± 0.47 wt % represented by 2-hydroxyethyl methacrylate (2HEMA) and tert-Butyl acrylate (tBA). Water absorption for pure crosslinkers ranged from 44.2 ± 2.7 wt % to 3.9 ± 1.2 wt % as poly(ethylene glycol) dimethacrylate $M_n$ 750 (PEGDMA750) and di(ethylene glycol) dimethacrylate (DEGDMA). The water absorption reached steady state for all synthesized polymers within approximately one day, and no

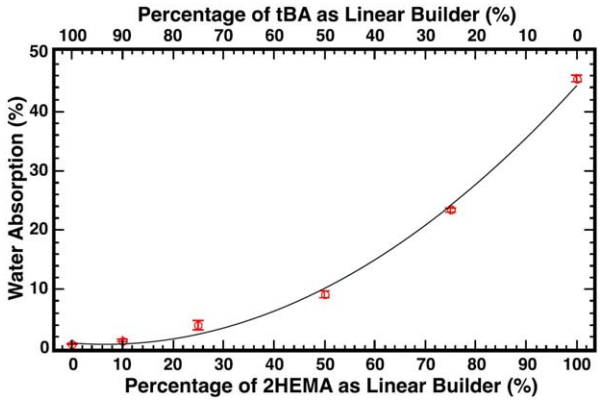


**Figure 4.** Twenty-four hour water absorption as a function of varying the relative weight ratio of tBA and 2HEMA in a system with a constant 5 wt % PEGDMA550. [Color figure can be viewed in the online issue, which is available at wileyonlinelibrary.com.]

degradation of polymers was seen within ten days except for 2-carboxyethyl acrylate (2CEA), which dissolved within 1 hr, and PPGA which lost approximately $6.0 \pm 2.7$ wt % of its original mass under aqueous conditions.

DMA results of the monofunctional fundamental systems displayed a wide range of glass transition characteristics, ranging from very broad transitions occurring over a large temperature range, such as 2-ethoxyethyl methacrylate (2EEM), to materials with sharp, stark transitions such as tBA. Under dry conditions tBA transitioned from the glassy regime to fully rubbery regime in around 20 °C. Transition temperatures were also important in consideration for future behavior. For example, considering the ultimate target transition region, the glass transition temperatures of poly(propylene glycol) acrylate (PPGA) were much too low, compared with tBA, which is close to the target region. This however is held with a caveat. It is known that water absorption, acting as a plasticizer, tends to drive down the transition temperature in a material.[56,57] Considering this, although 2HEMA has a glass transition temperature of 120 °C dry, it is expected to be much lower when saturated with water up to 54 wt %.

In addition, the multifunctional groups had worse transition behavior as the length between the active groups decreases or the number of number of active groups increases, that is, PEGMDA750, PEGDMA550, DEGDMA, and dipentaerythritol penta-/hexa-acrylate (DPPHA). This trend also tended to shift the overall storage moduli up, increase the transition temperature if visible, and decrease water absorption.

### Ternary Polymer Networks

Based on the results summarized in Table I, a combination of two linear builders, tBA and 2HEMA, were systematically varied relative to each other, while a small weight percentage of the crosslinker, PEGDMA550, and photoinitiator, 2,2-dimethoxy-2-phenyl-acetophenone (DMPA), were held constant at 5% and 0.5% of the total, respectively. Reflecting on Table I, tBA and 2HEMA individually absorbed relatively small and large amounts of water, respectively, while both maintained strong glass transitions—seen by the proximity of the onset and glass transition temperatures. Through varying the relative ratio of the two, the water absorption and the glass transition temperatures could be tailored. Water absorption as a function of the relative ratio of tBA and 2HEMA are reflected in Figure 4. Data points were taken at ratios containing 100/0, 90/10, 75/25, 50/50, 25/75, 0/100, tBA to 2HEMA for the 94.5 wt % linear builder. Data points represent the water absorption from an average of three samples, while error bars represent one standard deviation. The values increase non-linearly from nearly no water absorption to 45 wt % over the entire range tested as the ratio transitions from tBA to 2HEMA. In general, this behavior takes on a trend as represented by the best-fit line used to aid the eye in Figure 4; hinting that small changes in the weight percent ratio at higher concentrations of 2HEMA in the system will have larger effects on the relative amount of water absorbed when compared with lower concentrations.

DMA was also performed on the combinations of tBA/2HEMA ratios seen above, both under dry and aqueous conditions in order to observe the effect of water absorption on mechanical properties. Figure 5(a) displays representative curves of storage moduli with samples under ambient conditions. The glass moduli of the materials were relatively consistent ranging between approximately 2 and 3 GPa, while the rubbery modulus of the materials range from approximately 1–6 MPa. General trends observed as the monofunctional builder mixture transitioned from a low percentage of 2HEMA to a low percentage of tBA is an increase in the glass transition temperature and a gradual lengthening of the transition region.

Similarly, Figure 5(b) shows the results of DMA testing for samples after soaking for 24 hr. With increasing weight fraction of 2HEMA in the linear building mixture, the glass transition of the material decreases. This is indicative to the amount of water absorbed into the system. For example, as the 25/75 tBA-2HEMA material uptakes 23 wt %, shown in Figure 4, the glass transition changes from 87 °C in Figure 5(a) to 14 °C in Figure 5(b). Similarly, as the ratio of 2HEMA increased, effectively increasing the water absorption, the glassy modulus also tended to decrease in magnitude. At the extreme, with no tBA in the system, the modulus fell to slightly over 400 MPa soaked compared with over 3000 MPa for the same system when dry. In contrast, the relative magnitude of the rubbery moduli appears similar for the results between wet and dry. In summary, with an increase in the ratio of 2HEMA, water absorption also increased, which in turn lowered the glass transition, broadened the breadth of the transition region, and lowered the storage modulus in the glassy regime. Noting these characteristic behaviors as the ratio of the two linear builders transitions between tBA and 2HEMA allowed for a wide selection of glass transitions, material stiffness, and water absorption characteristics to choose from depending on the end application requirements.

### Final Polymer Network

With the groundwork laid, and the ability to select from a range of transition behaviors and water absorption characteristics, one polymer system was further investigated for use in final switchable surface. Parameters for further investigation were convenient for aqueous conditions and for showing the switchable

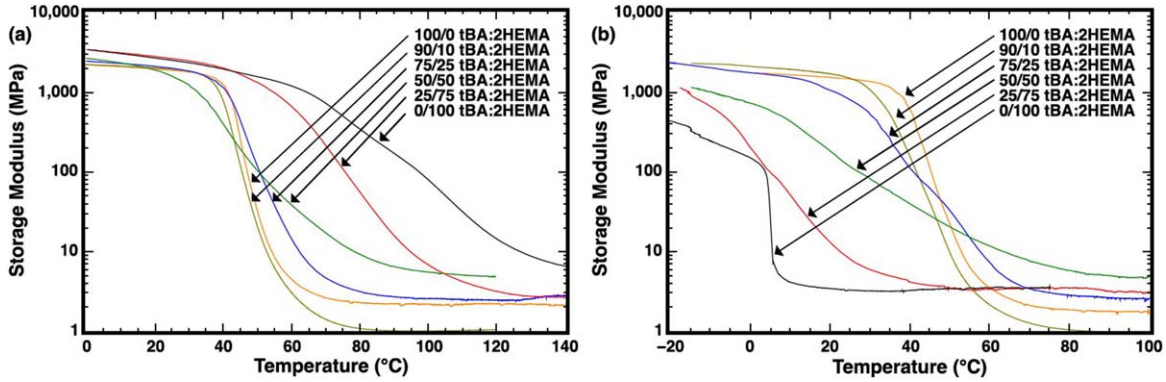


**Figure 5.** Representative (a) dry and (b) soaked DMA tests maintaining 5 wt % PEGDMA550, while varying the relative weight ratio of linear builders tBA and 2HEMA. [Color figure can be viewed in the online issue, which is available at wileyonlinelibrary.com.]

hydrophobic characteristics. These include temperatures initiating between 30 and 45 °C, a fast transition region such that the glass transition temperature followed within 20 °C of the onset temperature, while also having a minor degree of water absorption.

These designations ultimately aided in displaying the results on a research scale, but are also very reasonable characteristics for a variety of end applications, as the glassy regime is a typical temperature for standing water, while the target transition temperature region places the rubbery regime well below the boiling point of water under atmospheric conditions. Considering the set parameters, the final appropriate ternary network consisted of a linear building mixture of 9:1 by weight tBA and 2HEMA in a network of 94.5/5.0/0.5 wt % linear building mixture, PEGDMA550, and DMPA.

A representative curve from soaked DMA testing of the final network can be seen in Figure 6(a). Storage modulus is plotted on the left-hand axis in a logarithmic scale, while the material's tan delta is plotted on the right, both as a function of temperature. In the figure, the peak of the tan delta is used as to define the glass transition temperature. Similarly, the onset temperature is defined as the intercept of two tangent lines laid next to the plateau and transition regions at lower temperatures. The material is considered to be in the glassy regime below $T_{on}$, in the transition region between $T_{on}$ and $T_g$, and in the rubbery regime above $T_g$. Observing Figure 6(a), the storage modulus of the material decreased five orders of magnitude over the temperature range considered and is indicative of a transition of the material from its glassy regime at lower temperatures to its rubbery regime at the higher temperatures. Note that this temperature range also represents the normal range for a liquid-water state. Figure 6(a) reflects an onset temperature of 29.8 ± 4.4 °C and a glass transition temperature of 49.2 ± 2.2 °C.

Figure 6(b) represents stress-strain behavior under tension for the final network at a selection of temperatures around the materials transition from the glassy regime to the rubbery regime. The first temperature tested under tensile loading was well into the glassy region at 10 °C, followed by tests at a room temperature of 23 °C, close to the onset temperature, then near the glass transition temperature at 50 °C, and rounded off at 70 and 90 °C which have transitioned fully into the rubbery region of the material.

As a transition was made from the glassy to rubbery regime, the material reflects order of magnitude decreases in stiffness while maintaining appreciable ductility. Note that strain to failure was maximized around the glass transition temperature ($T_g = 49.2 \pm 2.2$ °C) while ultimate tensile strength and toughness were optimized around the onset temperature ($T_{on} = 29.8 \pm 4.4$ °C).

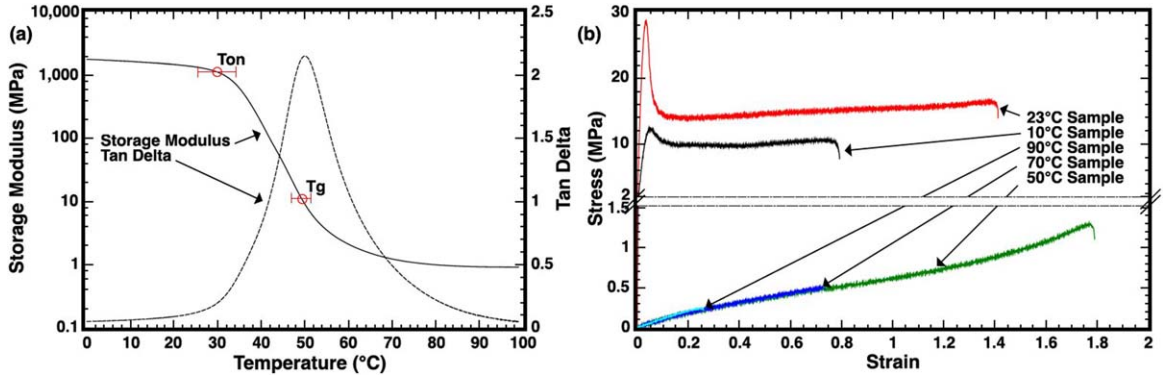


**Figure 6.** (a) Representative DMA curve of final ternary network along with the average $T_{on}$ and $T_g$ of the tests. (b) Tensile stress–strain behavior as a function of temperatures tested over the glass transition region. [Color figure can be viewed in the online issue, which is available at wileyonlinelibrary.com.]

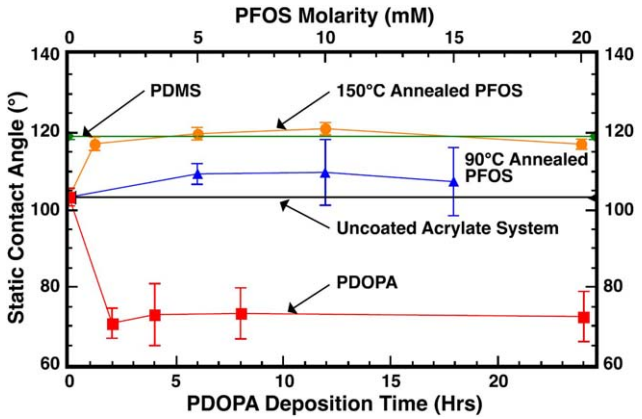


**Figure 7.** Contact angles of surface treatments considered for application on the pillar structure. [Color figure can be viewed in the online issue, which is available at wileyonlinelibrary.com.]

Tensile behavior generally matched what is expected for a lightly crosslinked acrylate thermoset.[42,56,57] In the glassy regime the material exhibited a stiff elastic region, yielding, and the onset of necking, where, at that point its ultimate tensile strength was reached. Beyond this strain, segmental chain elongation was occurring before fracture of the material. It is interesting to note that this behavior was optimized near the onset temperature, increasing both in the ultimate tensile strength and strain to failure between 10 °C and room temperature, while maintaining a very similar elastic region behavior. This result suggests that operating temperatures are optimized near the onset temperature when the material is to be operated in the stiff state.

On the opposite end of the spectrum, a slight variation of approximately 25 °C from the onset temperature fundamentally altered the character of system, transitioning to a much softer, pliable material, due to new polymer chain mobility. In addition, the elastic portion of the polymer was almost through the entire region to failure, comparable to elastomeric behavior. Similar to the glassy regime, there is an optimal operating temperature in the rubbery regime. When the samples were tested near the glass transition they showed a much higher strain to failure, decreasing, but ultimately following the same loading behavior as the temperature increased. The consequence of this fundamental alteration in the material's characteristic behavior was a strong, stiff material in the glassy regime that could thermally be transitioned over a short temperature range into a very ductile and easily deformable material. This fundamental change was used to elicit the alteration in the surface wettability.

### Surface Treatments

Various methods of surface treatments could be employed to alter the wettability of the surface of the acrylate, regardless of the acrylate's water absorption characteristics. Ultimately, this could allow for different surface characteristics spatially on the structured pillared surface, and, when used in conjunction with the thermally alterable polymer base, creating a switchable property. Three methods were investigated including polydopamine coating (PDOPA), trichloro(1H,1H,2H,2H-perfluorooctyl)silane coating (PFOS), and dip coating of Sylgard 184 silicone elastomer (PDMS). These investigations were performed exclusively on cast flat sheets of the final polymer system to separate any effects from the surface morphology.

Figure 7 displays the mean and one standard deviation of static contact angle results of PDOPA and PFOS surface coatings on flat sheets of the final acrylate system after soaking in water for 24 hr. Additionally in Figure 7 is a representation of a cast PDMS layer on top of the acrylate base, also soaked for 24 hr. For the PDMS a standard casting method was used, and no variations were considered, that is, displayed results are independent of either horizontal axis in the figure and are shown for comparison to the other treatment methods. Results of pure PDMS reflect similar results from Jin *et al.* who found static contact angles at 113°, while an angle of $119.0° \pm 0.8°$ was found here.[53] Note all PDOPA, PFOS, and PDMS results started with the uncoated acrylate material, displaying a contact angle of $103.3° \pm 2.3°$ that was then modified.

Contact angles from PDOPA as a function of deposition time are represented on the lower axis of Figure 7. Results of deposition were visible within 2 hr, and began to stabilize thereafter. At 24 hr the surface was lowered to a hydrophilic state displaying a contact angle of $71.4° \pm 6.5°$.

PFOS observations were made altering both the solution concentration and annealing temperature, corresponding to the top axis in Figure 7. The two curves of PFOS, annealed at 90 and 150 °C after the deposition process, follow a similar trend as a function of the concentration, being slightly optimized between a 5 and 10 m*M* while decreasing a small amount at 20 m*M*. However, the importance of annealing temperature is also highlighted in the curves as the contact angles at 10 m*M* solution increases from $109.7° \pm 8.5°$ to $121.0° \pm 1.6°$ with an increase in temperature from 90 to 150 °C. Therefore, PFOS annealed at 150 °C can be considered similar to the PDMS coatings, displaying a more hydrophobic state than the untreated acrylate.

### Combined Structured Surface

The final ternary polymer was cast into a structured surface as test samples using a direct molding process. After being removed from the mold the sample's pillars were distributed in a hexagonal pattern with a diameter of 1 mm and a depth of 3 mm (3:1 aspect ratio) with a packing factor of 3:1 diameters off pillar centers, as represented in Figure 3. This hexagonal array was continued such that the samples were five rows wide and covered approximately 30 mm in length.

A true color example of the sample's fabrication life cycle can be seen in Figure 8. Figure 8(a) displays the in-house mold in which the polymer system is cast. Subsequently the acrylate structure cast into a pillared array, shown in Figure 8(b), it could be subjected to PDOPA treatment over the entire surface. Results from this process can be also observed in Figure 8 by noting the color variation between (b) and (c), indicative of PDOPA deposition.[44] Finally, to create the hydrophobic pillar tops, samples were either dip coated in PDMS, producing a flanged top as shown in (d), or deposited with PFOS on the top surface, which resulted in no visible alterations (not shown in the figure).

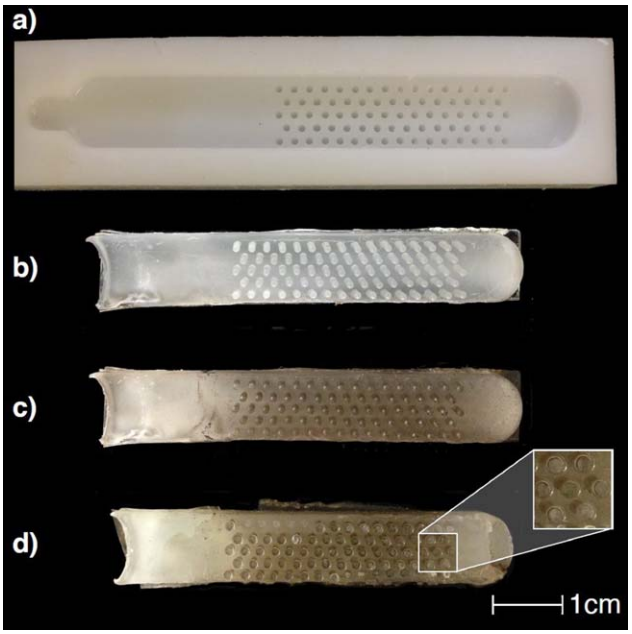


**Figure 8.** True color image of (a) the original mold, (b) acrylate system before surface treatment, (c) hydrophilic PDOPA coated surface, and (d) structure with hydrophobic PDMS tops (magnified two 2× in inset). [Color figure can be viewed in the online issue, which is available at wileyonlinelibrary.com.]

Optical results with close ups of the final structured surface at the various steps shown in Figure 8(b–d) and in contact with water droplets are displayed in Figure 9. For the images, samples at the various steps along the manufacturing processes were first presoaked, and subsequently dabbed to free surface water before placing a water drop on top. Water droplets were approximately 100 μL in size and were initially placed on the top surface of the pillars. Columns from right to left include the non-coated structured acrylate system, PDOPA coated throughout, PDOPA coated with PFOS topping, and PDOPA coated with flanged PDMS pillar tops. The first row displays the material in the original, non-deformed state, the second in the deformed state, and the third in the recovered state. The non-coated samples displayed a Wenzel state, with the drop remaining intact throughout all conditions. Surfaces with PDOPA coatings readily displayed hydrophilic effects, quickly dispersing the water over the entire surface in all states. For the final two columns, a Cassie–Baxter state was observed for both PFOS and PDOPA topped pillars when erect, while water dispersed into the remaining structure when deformed, fundamentally exhibiting the switchable nature. This process remains to be optimized based off a function of the geometry and size scale, as it was possible to see a transition between states based off external factors, however with droplets carefully applied, the results repeatedly showed the ability to transition between both the deformed and undeformed states.

## DISCUSSION

### Polymeric Base Network

A common theme between all of the base-polymer systems is an acryl group allowing for free radical polymerization to occur. On the other hand, the large variety of side group chemistry additional to these acryl groups and various chain lengths allow for a broad range of both water absorption and mechanical characteristics, as reflected in the results seen throughout Table I.

First, the water absorption characteristics of the monofunctional acrylates heavily followed the expected polarity of the systems such that the polar systems, 2HEMA, PPGA, and 2CEA, absorbed water or even degraded in the presence of water for the latter two. Conversely, the non-polar systems, tBA and 2EEM, had considerably less water absorption.[57–59]

Considering that both PPGA and 2CEA dissolved in fundamental water absorption studies neither were recognized as viable for the longevity of the system and abandoned in this study. Further compounding the degradation effects, PPGA also had a transition at temperature well below water's freezing temperature. 2HEMA was the natural choice to when comparing these three due to its high water absorption (∼50 wt %) and no degradation. When observing both the transition temperatures as well as absorption of 2EEM and tBA, both were similar at first glance, and remained as low water absorption linear building candidates. However, looking more closely, tBA exhibited a stronger glass transition region leading to a decrease in stiffness over a relatively narrow temperature region.

As the multifunctional candidates, recall that PEGDMA750, PEGDMA550, and DEGDMA, all essentially had the same molecular composition being terminated with two methacrylate groups but with decreasing amounts of ethylene glycol groups between the terminal ends. Observing the average molecular weight of the molecules in Figure 2 and noting the terminal end groups each have a gram molecular weight of approximately 85, this is approximately 13.5, 9, and 2 ethylene glycol groups, respectively. Therefore, water absorption was expected to decrease in conjunction with a reduction in free volume space, while glass transition regions were expected to elongate, and increase in transition temperature due to larger intermolecular reactions. Both these effects are also reflected in Table I. DPPHA was considered to have too many functional ends, with between 5 and 6 reactive acryl groups, resulting in poor thermo-mechanical characteristics under initial testing and was therefore abandoned. Based off the results seen here, PEGDMA550 was chosen based off its favorable transition characteristics, relative glass transition temperature, and modest water absorption as the crosslinking unit in the study.

The three materials selected from above were based explicitly on the fundamental needs for the final product designed in this article and was specifically chosen off their ability to be altered in combination. It must, therefore, be emphasized that a fundamental groundwork for the choice of an adequate base system was further investigated in combination to meet this need. With the selection of the three macromolecules to move forward with, tBA, 2HEMA, and PEGDMA550, a systematic approach to custom tailoring the glass transition properties and water absorption was taken; reflected in Figures 4 and 5.

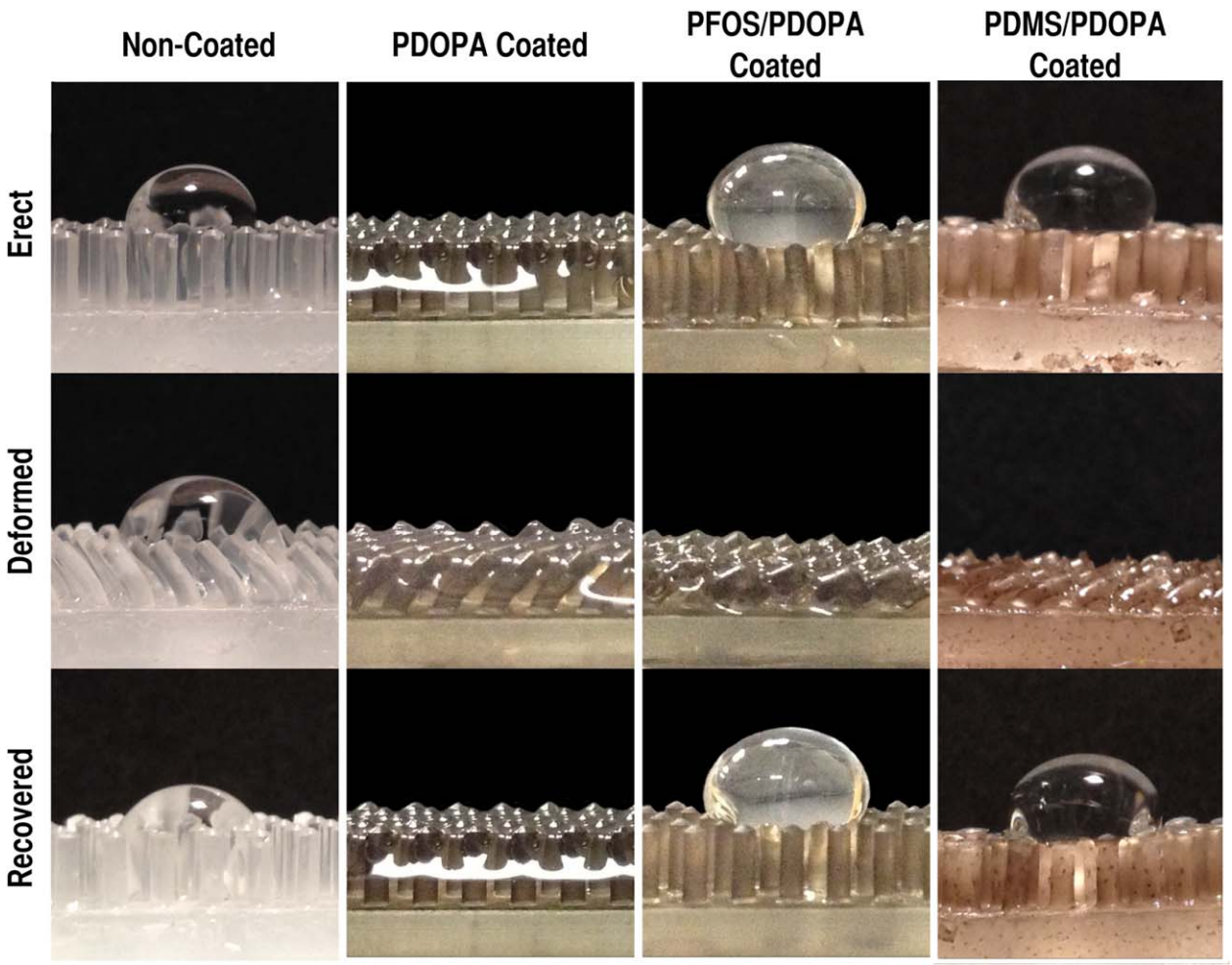


**Figure 9.** Qualitative results of water droplets in contact with structured acrylate system with various surface coatings (columns) in erect, deformed, and recovered conditions. [Color figure can be viewed in the online issue, which is available at wileyonlinelibrary.com.]

The effect of water absorption can be seen in the DMA results shown in Figure 5, where there was a directional change in the trend of glass transition temperatures compared with dry conditions. In dry conditions shown in (a), an increase in concentration of 2HEMA followed with an increased the glass transition temperature. Conversely, under wet conditions shown in (b), an increase in the amount of 2HEMA—and likewise water—effectively lowered the glass transition temperature quickly below the target point of 30–45 °C.

It also follows that the transition region, important for strong switchable behavior, broadened to its worst around 75/25 wt % tBA:2HEMA under wet conditions, seen in Figure 5. It is interesting to note that similar behavior between the dry and wet glass transition temperatures was seen in previous research by Lakhera *et al.*, where water absorption was tailored through variation of two monofunctional acrylates, benzyl acrylate and 2HEMA.[57]

For small amounts of 2HEMA in the system, the wet and dry glass transition temperatures follow similar a behavior to each other. As the amount of 2HEMA is increased a fundamental point is reached at 75/25 wt % tBA:2HEMA where the character changes substantially, and the soaked and dry glass transitions diverge from each other. This critical point is assumed to be due to the absorbed water overcoming secondary bonding between polymer chains. The Lakhera *et al.* article agrees with this, and notes that at higher than 5% water absorption (close to 75/25 wt % tBA:2HEMA) mechanical tensile results also become much poorer.[57]

Based off these observations, a final polymer network was chosen and consisted of a linear building mixture of 9:1 by weight tBA and 2HEMA in a network of 94.5/5.0/0.5 wt % linear building mixture, PEGDMA550, and DMPA. To further quantify the final network's characteristics, DMA and tensile test results were performed and are reflected in Figure 6. DMA results for the final structure suggest strong shape memory properties, such that a stark transition in the elastic modulus over a short temperature range between the onset temperature (30 °C) and glass transition temperature of 50 °C is observed. In this temperature range the elastic modulus decreases over two orders of magnitude, and up to three orders of magnitude by the time it reached fully into the rubbery regime. Alternative studies on similar polymer systems created by some of the authors, as well

as other groups have shown DMA behavior such as this to produce a strong shape memory characteristic behavior.[40,42] A dramatic change in mechanical behavior over this transition region can also be seen in the stress–strain behavior shown in part (b). For temperatures in the glassy regime, materials display plastic behavior with significant ductility, while materials in the rubbery regime display hyperelastic behavior. This fundamental change in mechanical behavior is due to the increase in free volume space in the polymer, relaxing steric effects between polymer chains. The practical effect is a stiffer, stronger, yet less elastically ductile product in the glassy regime, while in the rubbery regime you have a very ductile and low stiffness material that can easily bend and fold under low loads.

Of particular interest in Figure 6 are the temperatures where maximum strength and ductility were reached. The material is found to be the strongest near its onset temperature at 23 °C, and also shows relatively high strain to failure at this temperature as well. In its rubbery state, the material is found to reach its highest strain to failure near the glass transition temperature at 50 °C. A high strain to failure in this transition region is found to be the case in similar works by Yakacki *et al.*, shown to be optimized when a low amount of crosslinker is used in the system.[42] It is also interesting to note that at temperatures past the glass transition the ductility of the material decreases as temperature is increased; yet the stress–strain behavior apparently follows the same characteristic path, just failing sooner than its lower temperature counterparts in the rubbery regime. Therefore, operating at or near the onset transition when a stiff polymer system is required can optimize the overall toughness of the polymer. Then, when a pliable material is needed, it can be optimized by simply heating the system slightly past the glass transition temperature, significantly decreasing the stiffness, while still improving the strain to failure when compared with higher temperatures.

### Preferential Surface Treatments

The addition of surface treatments to the tailored acrylate system allowed for custom alteration of surface properties without changing the behavior of the acrylate substructure. Ultimately, this permitted water absorption in the acrylate to remain low, while having the favorable surface interactions for the switchable structured surface. Three different surface treatment investigations, displayed in Figure 7, allow a myriad of options for the particular combination in the final pillared surface. As a proof-of-concept design, the acrylate was formed with a hydrophilic foundation on the acrylate base and pillar sides using PDOPA, but with hydrophobic tops, either structured with PDMS flanges, or a simple PFOS coating. This development is shown in Figure 8. As is, operation with erect pillars encourages a hydrophobic surface, with a hydrophilic structure being exposed during elevated water temperatures. However, this combination could easily be switched, coating the substructure in PFOS, and topping with PDOPA, reversing the characteristics.

### Multitiered Surface Structure

The final structured surface shown here was a proof-of-concept design showing the possibility of a structured, switchable hydrophobic surface, through surface treatments and a thermo-mechanical acrylate base. In the combination displayed here, a surface such as this cast onto a water treatment membrane would prevent suspended solids from depositing on, and subsequently adhering, to the active layer of the membrane surface during normal operating conditions. Through custom designing the shape memory polymer for the specific purpose, water temperatures can be maintained in a comfortable region with temperature range between freezing and the onset temperature of 29.8 ± 4.4 °C for normal operation with the mechanical properties of the water being optimized at the onset temperature. During the cleaning process, the water would simply need to be heated above the glass transition temperature of 49.2 ± 2.2 °C, inducing a more flexible polymer, exposing the hydrophilic undercarriage. In this regime, adhesive interactions between the membrane surface and suspended debris in the water would be minimalized as a result of the higher affinity of the surface for water. This would result in the debris being removed from the system by hydraulic shearing. Removal of any force at elevated temperatures, that is, pressure, would allow the shape memory polymer to return to its erect state for normal operation.

Qualitative results displayed in Figure 9 show the proof-of-concept character, and demonstrate the importance of the combined effects in the multitiered structure. These include the mechanical robustness of the polymer system developed so it can transition between states reliably and recover the structuring of the surface to allow for different wetting states through multiple cycles. This also highlights the importance of the combination of surface treatments. Future investigation will need to be made to optimize geometrical design and size to maximize the switchable effect, through alterations in the surface treatment locations.

## CONCLUSIONS

In this study, the groundwork for a multitiered surface construct was created to allow for alterations in the surface wettability. This was done through the *combination* of a smart-surface understructure patterned into an array, on which selectively placed chemical surface treatments were made. To do this, first a customized acrylate-based polymer was constructed through the use of a systematic study varying base constituents chosen from a selection of commercially available acryl-based macromolecules. They were methodically varied and investigated for water absorption and mechanical stiffness under dry and aqueous conditions over a range of temperatures, allowing for a range of transition and water absorption characteristics as needed for an end application. Further, the polymer system was dialed to have target mechanical properties under submerged conditions, and was shown to have the ability to be photopolymerized into a pillared surface structure. This polymer structure could be altered between an erect and bent state. Three surface treatments, two hydrophobic in nature and one hydrophilic in nature, were investigated using basic water contact angle tests when affixed to a flat casting of the acrylate-based subsystem. These surface treatments, including PDOPA, PFOS, and PDMS were then selectively placed on the pillared surface such that hydrophobic portions (PFOS and PDMS) were exposed at the surface when erect, and hydrophilic portions (PDOPA) were

exposed when the pillars were bent over, displaying the proof of concept switchable nature.

## ACKNOWLEDGMENTS

This research was supported by the University of Wyoming Office of Water Programs funded jointly by the USGS, the Wyoming Water Development Commission, and the University of Wyoming.

## REFERENCES

1. Nishimoto, S.; Bhushan, B. *RSC Adv.* **2013**, *3*, 671.
2. Banerjee, I.; Pangule, R. C.; Kane, R. S. *Adv. Mater.* **2011**, *23*, 690.
3. Genzer, J.; Efimenko, K. *Biofouling* **2006**, *22*, 339.
4. Yebra, D. M.; Kiil, S.; Dam-Johansen, K. *Prog. Org. Coat.* **2004**, *50*, 75.
5. Liu, Y.; Ai, K.; Lu, L. *Chem. Rev.* **2014**, *114*, 5057.
6. Yao, X.; Song, Y.; Jiang, L. *Adv. Mater.* **2011**, *23*, 719.
7. Yue, M.; Zhou, B.; Jiao, K.; Qian, X.; Xu, Z.; Teng, K.; Zhao, L.; Wang, J.; Jiao, Y. *Appl. Surf. Sci.* **2015**, *327*, 93.
8. Yu, H. Y.; Hu, M. X.; Xu, Z. K.; Wang, J. L.; Wang, S. Y. *Sep. Purif. Technol.* **2005**, *45*, 8.
9. Kim, K. S.; Lee, K. H.; Cho, K.; Park, C. E. *J. Memb. Sci.* **2002**, *199*, 135.
10. Ulbricht, M.; Belfort, G. *J. Memb. Sci.* **1996**, *111*, 193.
11. Callow, M. E.; Callow, J. A.; Ista, L. K.; Coleman, S. E.; Nolasco, A. C.; Lopez, G. P. *Appl. Environ. Microbiol.* **2000**, *66*, 3249.
12. Ista, L. K.; Mendez, S.; López, G. P. *Biofouling* **2010**, *26*, 111.
13. Jeon, S. I.; Lee, J. H.; Andrade, J. D.; De Gennes, P. G. *J. Colloid Interface Sci.* **1991**, *142*, 149.
14. Barthlott, W.; Neinhuis, C. *Planta* **1997**, *202*, 1.
15. Shahsavan, H.; Arunbabu, D.; Zhao, B. *Macromol. Mater. Eng.* **2012**, *297*, 743.
16. Nosonovsky, M.; Bhushan, B. *Ultramicroscopy* **2007**, *107*, 969.
17. Petronis, S.; Berntsson, K.; Gold, J.; Gatenholm, P. *J. Biomater. Sci. Polym. Ed.* **2000**, *11*, 1051.
18. Schumacher, J. F.; Carman, M. L.; Estes, T. G.; Feinberg, A. W.; Wilson, L. H.; Callow, M. E.; Callow, J. A.; Finlay, J. A.; Brennan, A. B. *Biofouling* **2007**, *23*, 55.
19. Zorba, V.; Stratakis, E.; Barberoglou, M.; Spanakis, E.; Tzanetakis, P.; Anastasiadis, S. H.; Fotakis, C. *Adv. Mater.* **2008**, *20*, 4049.
20. Bhushan, B. *Philos. Trans. R. Soc. A Math. Phys. Eng. Sci.* **2009**, *367*, 1445.
21. Cassie, A. B. D.; Baxter, S. *Trans. Faraday Soc.* **1944**, *40*, 546.
22. Wenzel, R. N. *J. Ind. Eng. Chem. (Washington, D.C.)* **1936**, *28*, 988.
23. Patankar, N. A. *Langmuir* **2004**, *20*, 7097.
24. Marmur, A. *Langmuir* **2006**, *22*, 1400.
25. Wang, R.; Hashimoto, K.; Fujishima, A.; Chikuni, M.; Kojima, E.; Kitamura, A.; Shimohigoshi, M.; Watanabe, T. *Nature* **1997**, *388*, 431.
26. Lee, H.; Lee, B. P.; Messersmith, P. B. *Nature* **2007**, *448*, 338.
27. Bhushan, B.; Sayer, R. A. *Microsyst. Technol.* **2006**, *13*, 71.
28. Ueda, E.; Levkin, P. A. *Adv. Mater.* **2013**, *25*, 1234.
29. Pan, S.; Guo, R.; Xu, W. *Soft Matter* **2014**, *10*, 9187.
30. Hua, Z.; Yang, J.; Wang, T.; Liu, G.; Zhang, G. *Langmuir* **2013**, *29*, 10307.
31. Rajkumar, K.; Rajendrakumar, R. T. *Plasma Chem. Plasma Process* **2013**, *33*, 807.
32. Ista, L. K.; López, G. P. *J. Ind. Microbiol. Biotechnol.* **1998**, *20*, 121.
33. Ista, L. K.; Pérez-Luna, V. H.; López, G. P. *Appl. Environ. Microbiol.* **1999**, *65*, 1603.
34. Zhang, S.; Liu, Z.; Bucknall, D. G.; He, L.; Hong, K.; Mays, J. W.; Allen, M. G. *Appl. Surf. Sci.* **2011**, *257*, 9673.
35. Jiang, B.; Zhang, L.; Liao, B.; Pang, H. *Polymer* **2014**, *55*, 5350.
36. Wu, Z. L.; Buguin, A.; Yang, H.; Taulemesse, J. M.; Le Moigne, N.; Bergeret, A.; Wang, X.; Keller, P. *Adv. Funct. Mater.* **2013**, *23*, 3070.
37. Lin, P. C.; Yang, S. *Soft Matter* **2009**, *5*, 1011.
38. Chen, C. M.; Yang, S. *Adv. Mater.* **2014**, *26*, 1283.
39. Yakacki, C. M.; Shandas, R.; Safranski, D.; Ortega, A. M.; Sassaman, K.; Gall, K. *Adv. Funct. Mater.* **2008**, *18*, 2428.
40. Lakhera, N.; Laursen, C. M.; Safranski, D. L.; Frick, C. P. *J. Polym. Sci. Part B Polym. Phys.* **2012**, *50*, 777.
41. Safranski, D. L.; Lesniewski, M. A.; Caspersen, B. S.; Uriarte, V. M.; Gall, K. *Polymer* **2010**, *51*, 3130.
42. Yakacki, C. M.; Willis, S.; Luders, C.; Gall, K. *Adv. Eng. Mater.* **2008**, *10*, 112.
43. Waite, J. H.; Tanzer, M. L. *Science* **1981**, *212*, 1038.
44. Lee, H.; Dellatore, S. M.; Miller, W. M.; Messersmith, P. B. *Science* **2007**, *318*, 426.
45. Liao, Y.; Wang, Y.; Feng, X.; Wang, W.; Xu, F.; Zhang, L. *Mater. Chem. Phys.* **2010**, *121*, 534.
46. Silberzan, P.; Léger, L.; Ausserré, D.; Benattar, J. J. *Langmuir* **1991**, *7*, 1647.
47. Chen, J.; Ko, F. H.; Hsieh, K. F.; Chou, C. T.; Chang, F. C. *J. Vac. Sci. Technol. B, Microelectron. Process. Phenom.* **2004**, *22*, 3233.
48. Zhang, M.; Wu, J.; Wang, L.; Xiao, K.; Wen, W. *Lab Chip* **2010**, *10*, 1199.
49. Cho, Y. S.; Ahn, S. H.; Lee, S. H. *J. Korean Phys. Soc.* **2013**, *63*, 218.
50. McCloskey, B. D.; Park, H. B.; Ju, H.; Rowe, B. W.; Miller, D. J.; Chun, B. J.; Kin, K.; Freeman, B. D. *Polymer* **2010**, *51*, 3472.
51. Arena, J. T.; McCloskey, B.; Freeman, B. D.; McCutcheon, J. R. *J. Memb. Sci.* **2011**, *375*, 55.

52. Carman, M. L.; Estes, T. G.; Feinberg, A. W.; Schumacher, J. F.; Wilkerson, W.; Wilson, L. H.; Callow, M. E.; Callow, J. a.; Brennan, A. B. *Biofouling* **2006**, *22*, 11.

53. Jin, M.; Feng, X.; Xi, J.; Zhai, J.; Cho, K.; Feng, L.; Jiang, L. *Macromol. Rapid Commun.* **2005**, *26*, 1805.

54. Kanungo, M.; Mettu, S.; Law, K. Y.; Daniel, S. *Langmuir* **2014**, *30*, 7358.

55. Hossfeld, C. K.; Schneider, A. S.; Arzt, E.; Frick, C. P. *Langmuir* **2013**, *29*, 15394.

56. Smith, K. E.; Parks, S. S.; Hyjek, M. A.; Downey, S. E.; Gall, K. *Polymer* **2009**, *50*, 5112.

57. Lakhera, N.; Smith, K. E.; Frick, C. P. *J. Appl. Polym. Sci.* **2012**, *128*, 1913.

58. Corkhill, P. H.; Jolly, A. M.; Ng, C. O.; Tighe, B. J. *Polymer* **1987**, *28*, 1758.

59. Raj Singh, T. R.; McCarron, P. A.; Woolfson, A. D.; Donnelly, R. F. *Eur. Polym. J.* **2009**, *45*, 1239.